J Ther Eng, Vol. 11, No. 2, pp. 390−406, March, 2025

Journal of Thermal Engineering
Web page info: https://jten.yildiz.edu.tr
DOI: 10.14744/thermal.0000922

Journal of Thermal Engineering

Research Article

Enhancing heat efficiency in arid environments using a PVT collector for revealed facade shelter

Mohamed Cherif BENZID[1,2], Boubekeur DOKKAR[1,2,*], Abdelghani BOUBEKRI[1]

[1]Department of Mechanical Engineering, University of Kasdi Merbah, Ouargla, 30000, Algeria
[2]Laboratory of Applied Mechanics and Energy Systems, University of Kasdi Merbah, Ouargla, 30000, Algeria

ARTICLE INFO

Article history
Received: 03 April 2024
Revised: 08 July 2024
Accepted: 09 July 2024

Keywords:
Desert Climate; Discovered Façade Shelter; Heating; PVT Collector

ABSTRACT

In Ouargla neighboring (Algeria), the harsh climate conditions and the isolation of agricultural areas pose some difficulties for developing agriculture. For lightening climatic constraints, thermal comfort in farmer homes is required. The present study investigated the thermal behavior in a 3D model of an existing earth-sheltered room using Ansys Software. To improve room heating on the coldest winter day, different room designs are investigated. The variant equipped with a photovoltaic-thermal (PVT) solar collector shows significant thermal comfort, where for an ambient temperature of around 4°C, the indoor temperature in the living space reaches about 24°C. Also, the PVT system has a low initial cost compared to a heat pump, where the gap reaches 1460 euros. In addition, the long-term exploitation of discovered façade shelters achieves an appreciable benefit against the mode of farmers' transportation between the city and the farm.

Cite this article as: Benzid MC, Dokkar B, Boubekri A. Enhancing heat efficiency in arid environments using a PVT collector for revealed facade shelter. J Ther Eng 2025;11(2):390−406.

INTRODUCTION

The southern Algerian region is characterized by a desert climate with hot summers and cold winters, and lack of an electricity grid in isolated areas. These constraints contribute in farmers' suffering to find comfortable shelters for taking rests. This situation requires a suitable solution to improve shelter thermal comfort using solar energy systems in off-grid areas. In paricular, the winter season is characterized by the critical period for harvesting and treating palm trees. Certain cultural areas contain abandoned rooms excavated in hills and used as homes for small family workers since decades ago; they can be adjusted and transformed into temporary shelters. In the available literature, this home style is less studied where there are only works concerning the heating of ordinary buildings with passive systems using thermal solar energy. They use free solar radiation as vital energy source for heating and cooling [1]. Many researchers tend toward studying the feasibility of these systems in terms of effectiveness and investment cost. The Trombe wall, covered with an external glazing layer, is the most well-established technique in this field; it consists of storing solar energy on a large wall used after sunset. R. Elghamrya and Hassana [2] investigated an experimental work in New Borg El Arab City, Alexandria (Egypt) by using a Trombe wall (TW) combined with a geothermal air tube (GT) or/

***Corresponding author.**
*E-mail address: boubekeur.ogx@gmail.com

This paper was recommended for publication in revised form by Editor-in-Chief Ahmet Selim Dalkılıç

and solar chimney (SC) including photovoltaic panel (PV). The results indicate that natural renewable energy systems can increase the room temperature to a maximal value of about 14°C and change the room air to a maximal value of about 58 times per day. The heating performance of an improved Trombe wall is experimentally studied by Dong et al. [3]. The results indicate that the indoor air temperature is above 16°C, and the minimal air velocity is 0.35 m/s at the vent outlet. Also, the daily thermal efficiency of the upgraded T-Wall is over 50% during the day. For other techniques, there are solar thermal collectors. These collectors are the main components of any solar energy system; they receive and convert solar radiation into heat energy. Then, they transfer this energy via a working fluid for different uses [4]. Agathokleous et al. [5] studied the energy performance of a flat-plate solar thermal air collector integrated into office space in three weather zones: Freiburg, Naples, and Almeria. The results show that by supplying the generated hot air into the heating, ventilation, air conditioning system, and clothes dryer, the primary energy savings are always realized. By considering only the passive effects, improvement in thermal comfort is obtained in cold areas (Freiburg), and for East-oriented collectors in temperate climates (Naples). Buonomano et al. [6] studied the thermodynamic behavior of a flat-plate solar thermal collector design for building integration, using water as a working fluid. As a result, the passive effects analysis shows that the winter-free heating impact enables meaningful drops in heating building demand. Also, only in the coldest climatic areas (London, Freiburg, and Prague), do passive effects lead to energy savings on an annual basis. For providing moderate temperature in commercial buildings for HVAC purposes, the feasibility of a novel, low-profile concentrated solar thermal collector has been examined by Li et al. [7]. They aim to reduce the levels of non-renewable energy consumption. Also, the proposed collector is getting close to being economically viable for solar heating and cooling applications. Integrating a few upgrades can provide about 50% of the building's cooling and heating needs in Sydney (Australia). 3 m^2/kW as a specific collector area is required for this improved collector. Miao et al. [8] studied experimentally an innovative design of solar thermal collectors for a dual purpose. They accomplish heat and cold collection using solar heating and night sky cooling. The results show that based on solar radiation in the late afternoon (about 14:00) of a summer day with a clear sky in Fargo (North Dakota, USA), the collector's heating capacity is 505.0 ±7.8 W/m^2. For eventual high radiation, a subtantial heat collection capacity can be expected. To reduce the fossil primary energy demand in high rise buildings, transparent solar thermal collectors have been integrated into their facades and studied numerically by Maurer et al. [9]. Mainly, they found that a high-rise building may reach around 20% of its overall heating and cooling energy demand with renewable energy. This energy level can be supplied if the building has TSTCs installed on 20% of its east, west, and south façade areas. There is also a common passive system in the HVAC field, which is the solar chimney. The operational concept of solar chimneys and the T-walls have covered structures. They convert thermal energy into kinetic energy of moving air. The ventilation fan blows hot air into the building; it can provide airflow for cooling or heating purposes [10]. Also, the solar chimney is used for electricity generation, Haghighi and Maerefat [11] studied solar chimney ability to meet the required thermal and ventilation needs during winter days. They examine heat transfer by natural convection and surface radiation of a ventilated room in contact with a cold external environment. The results show that for a room with weak solar radiation of 215 W/m^2 and a low ambient temperature of 5°C, the system can deliver good air conditioning (heating) during the day. In China, Hong et al. [12] used EnergyPlus to examine the energy performance of a solar chimney (SC) integrated into high performance for a two-story detached house. The results show that most of the year, the SC provides ventilation rates higher than the minimal necessary rate. In general, 549.0 kWh or 9.0% of the total HVAC energy consumption is estimated as an annual energy saving of the SC for the studied house. The thermal behaviors of a solar chimney combined with organic phase change material (PCM) under different heat fluxes have been studied by Li and Liu [13]. The results show that the system performance rapidly declines if the heat flux is less than 500 W/m^2, but it doesn't significantly increase once it exceeds 700 W/m^2. However, the chimney performance under low radiation can be further enhanced by applying highly effective thermal conductivity enhancers.

Recently, nano-fluids have been introduced to enhance the efficiency of thermal collectors. Mohammed et al. [14] provided a comprehensive review of the scientific advancements regarding the use of nano-fluids in flat-plate solar collectors (FPSCs). Their findings indicate that previous studies demonstrate the successful application of nano-fluids in improving FPSC efficiency. However, nano-fluids exhibit higher pressure drops against conventional liquids, and these pressure drops, along with the required pumping power, increase with the volume flow rate. Qader et al. [15] investigated the efficiency and environmental benefits of solar energy, focusing on the thermal efficiency, exergy, and entropy of solar collectors. Their experiment utilizes two glass-topped collectors, fluid transfer tubes, and aluminium heat-absorbing plates, with glass wool insulation to minimize heat loss. They prepared a 0.5% TiO_2/water nano-fluid using a mechanical and ultrasonic stirrer. The results indicate that solar radiation increases thermal efficiency up until midday. Filtered water produces 380 W and 395 W of energy in March and April, respectively, while the nano-fluid increases the energy output to 395 W and 415 W. Additionally, porous media can enhance heat flux. Qader et al. [16] investigated forced convection heat transfer in a horizontally heated circular pipe using a porous medium of stainless-steel balls. They applied heat flux rates of 6250 and 12500 W m^{-2}. The simulation results

demonstrate increased turbulence and eddy formation. The Nusselt number increases with ball diameters of 1–3 mm, rising by 46.7% for Reynolds numbers between 3200 and 6500, and by 4.36% for heat flux rates between 6250 and 12500 W m^{-2}.

The articles below deal with the thermal comfort in ordinary houses with conventional architecture, and they analyze the different techniques applied to improve solar collector efficiency. However, the present study treats the thermal comfort of new home design which combines the direct effect of geothermal energy with solar energy in a desert climate. This home consists of an old shelter excavated inside a cohesive soil hill. A solar thermal collector is integrated into this shelter for daily heating. To provide electricity to the ventilation fan, a photovoltaic panel is added to the thermal collector to form a PVT solar collector. This collector presents a free shelter heating in the off-grid Ouargla region. A 3D model is simulated using Ansys CFD code, where the base case results are validated by the experimental measurements. The exploitation of this shelter can help the farmers to take rests and reduce the daily transportation charge of round trips between the city and the farms.

MATERIALS AND METHODS

Description of the Shelter

The shelter is located in the province of Ouargla (Algeria), according to the coordinates: Latitude: 31.9500 and Longitude: 5.3167 [17]. This region is characterized by a hot and arid summer, and a cold and dry winter. The sky is mostly clear with rare clouds; the statistics show that the extreme temperatures reached −3.7°C in January and 53.5°C in August [18, 19].

The shelter consists of an old room excavated inside the cohesive soil of a hill; it is oriented towards the north direction to decrease the sun rays exposition. The shelter position gives good opportunities to explore the geothermic and shade advantages to reduce the effect of ambient temperature. The internal wall surfaces are covered with a small plaster layer that doesn't affect the thermal comfort and makes a beautiful white internal shelter view.

Figure 1a presents the shelter façade contains:

- Shelter entrance: a big opening excavated in the shelter façade allows an average tall person to enter inside the shelter.
- Aeration hole: A small opening excavated on the left side of the entrance ensures the aeration of the shelter.

Figure 1b shows the internal shelter view with a chimney opening at the bottom of the lateral shelter wall. The chimney opening allows feed firewood embers for reinforcing night shelter heating by burning palm solid residues. Figure 2 shows the internal shelter design with its curved roof and the shelter dimensions.

Mathematical Model

In this study, to develop a simple and quick-to-handle formulation of the three-dimensional mathematical model in mixed convection phenomenon, the following hypotheses are adopted:

- The flow regime is laminar.
- The air is considered a Newtonian fluid.
- Radiation heat transfer is negligible inside the shelter.
- There are no indoor chemical reactions or internal heat sources.

a) b)

Figure 1. The excavated shelter: a) external view, b) internal view.

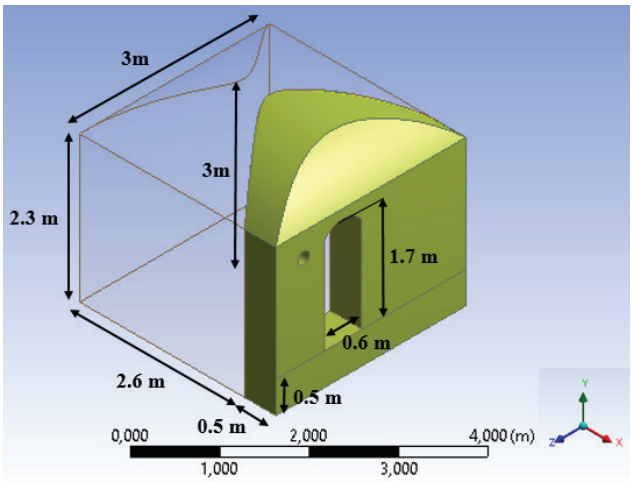

Figure 2. Shelter design and dimensions.

- All the thermos-physical properties are constant and evaluated at a reference temperature.

Concerning the fluid variation density, the Boussinesq approximation is applied, where the approach generally has the following assumptions:

1. Fluid density is constant except for the buoyancy term.
2. The remaining properties of the fluid are constant.
3. Viscous dissipation is negligible.

The first point notifies that the continuity equation has an incompressible form, and the density is considered variable only in the gravitational term of the momentum equation. Therefore, the equation describing the density variation is written as follows:

$$\rho = \rho_0[1 - \beta_T(T - T_0)] \quad (1)$$

Where; ρ_0 is the fluid density at the reference temperature T_0, T is the temperature of the fluid for any point in confined space and β_T is the coefficient of thermal volumi-nal expansion of the fluid given by the following relation:

$$\beta T = -\frac{1}{\rho_0}\left(\frac{\partial \rho}{\partial T}\right)_P \quad (2)$$

With; P is the pressure.

In general, a decrease in fluid density is caused by increasing temperature. The Boussinesq approximation is valid as long as the density variations are less than 10 % of the average density magnitude ($\Delta\rho / \rho \leq 0.1$) [20].

The airflow in the shelter is governed by the following mathematical equations, which are respectively the continuity equation, motion equation, and energy equation [21]:

$$\frac{\partial \rho}{\partial t} + div(\rho.\vec{V}) = 0 \quad (3)$$

$$\frac{D(\rho\vec{V})}{Dt} = \rho\vec{g} - \vec{\nabla}P + \mu\nabla^2\vec{V} \quad (4)$$

$$\rho Cp\frac{\partial T}{\partial t} = \vec{\nabla}.(\lambda\,\vec{\nabla}T) + q \quad (5)$$

Where: ρ is the fluid density, $\vec{V}$ is the fluid velocity vector, $\vec{g}$ is the gravity acceleration, $\vec{\nabla}P$ is the pressure gradient, μ is the dynamic viscosity, ∇^2 is the Laplace operator, Cp and λ are respectively the calorific capacity and thermal conductivity of the fluid, T is the fluid temperature and q is heat source term.

Boundary Conditions

Since the shelter is an underground cavity, the wall temperatures (except the façade wall) obey the soil temperature law, which depends on the depth. In literature, there are different models to determine the earth's temperature, such as the studies of Cherrad et al. [22] and Belatrache et al. [23]. In this work, the mathematical model given by Derbal and Kanoun [24] is adopted to determine the boundary temperatures (see the model details in the appendix).

Numerical Simulation and Mesh Optimization

The mathematical model consists of nonlinear coupled differential equations. So, the resolution requires a CFD code such as ANSYS software. The shelter geometry is drawn in three dimensions and the boundary conditions of lateral walls are introduced as calculated with the model mentioned above in the previous subsection. The summer maximal ambient temperature is chosen as boundary conditions of the external façade surface. SIMPLE algorithm is used to treat the coupling between pressure and velocity. The governing equations are discretized using the second-order upwind method. An under-relaxation coefficient is included to accelerate the iterations. The value of 10-6 is fixed as a residual error for the different parameters.

The triangular mesh is chosen to facilitate the location of the mesh nodes on the curved shelter roof (Fig. 3). The choice of the mesh number must satisfy the assumption that the information at the nodes must present the solution in the entire domain with a less difficult task [25]. The

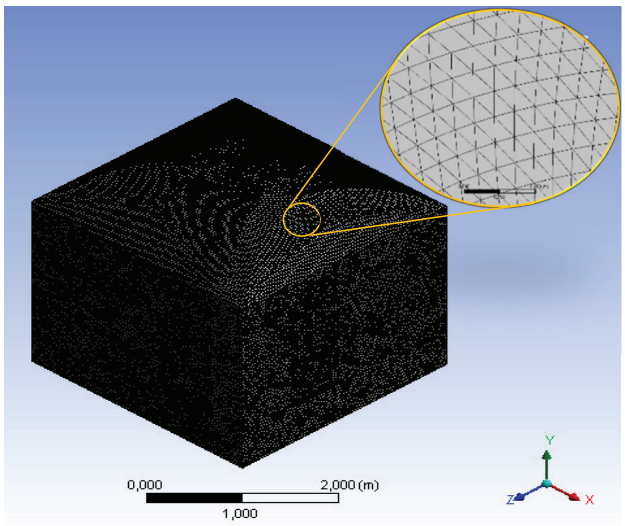

Figure 3. Meshing of computational domain.

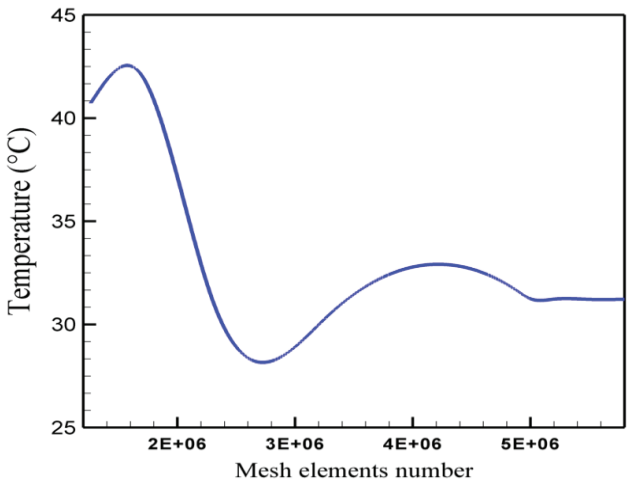

Figure 4. Indoor temperature at shelter middle.

best mesh is achieved using the temperature variation in the room middle according to the mesh element number. Figure 4 indicates that the temperature can be considered meshing independent starting from 4889594 meshes with an absolute relative error of less than 10-3.

Process of the Shelter Heating Improvement

For improving the shelter heating, the thermal behavior is treated in three shelter cases: base case, door closed case, and with the integration of photovoltaic thermal (PVT) collector. Figure 5 shows the shelter location (as described above in the subsection "description of the shelter ") with the different approach steps of the shelter heating improvement.

Shelter base case

In this case, the original shelter is kept without modification (Fig. 6). The shelter's door is open. The façade is oriented to the north and isn't exposed to sun rays; it is affected only by ambient temperature. For the remaining

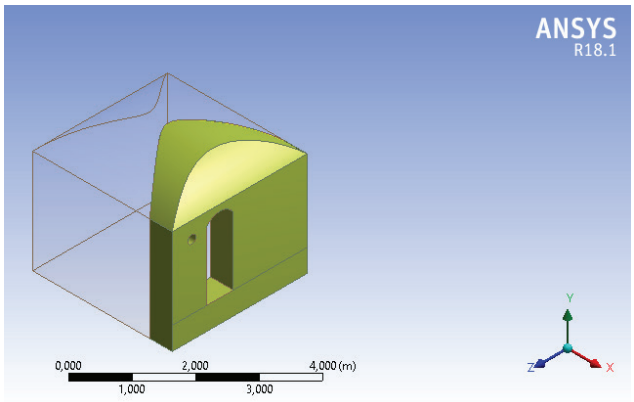

Figure 6. Base case of the original shelter.

shelter walls, the earth temperature is taken as boundary conditions.

Shelter with a closed door

The difference between the shelter base case and this second case is that a wooden shelter door is added to reduce the external cold air penetration inside the shelter. A small hole is added under the door to allow shelter aeration, and all shelter designs are illustrated in Figure 7.

Shelter with a PVT collector

In this case, a PVT solar collector is added (Fig. 8). The collector design and dimensions are given by the study of Khenfer et al. [26]. The PVT collector is placed on the west side of the facade to take advantage of the short distance from the door. A 5 meters PVC pipe with 10 cm of diameter connects the shelter to the collector. This pipe is considered thermally insulated and has the following thermo-physical parameters: $\rho = 1.38\ g.cm^{-3}$, $C = 1046\ J/kg.K$, $\lambda = 0.2\ W/m.K$.

Also, the pipe end is equipped with an air extractor and connected at the shelter bottom to suck in the hot air produced by the solar collector. The electricity of the PV panel

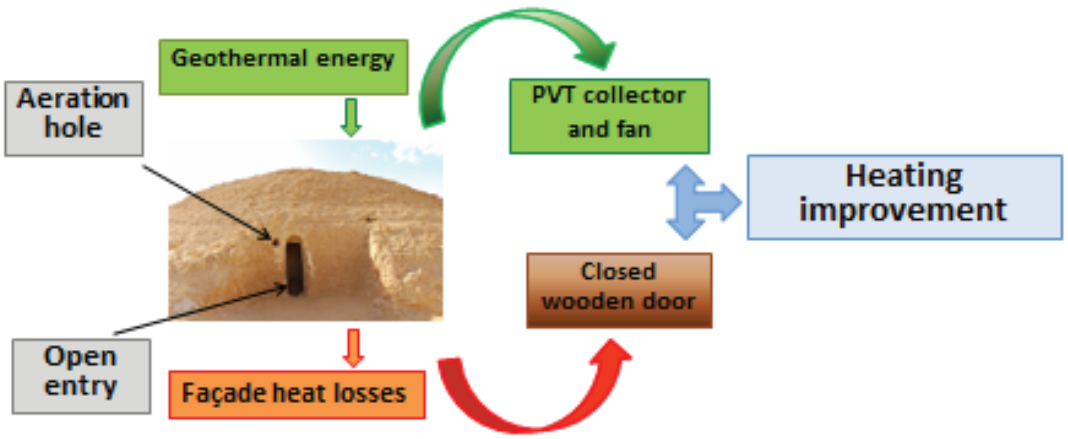

Figure 5. Approach of heating improvement.

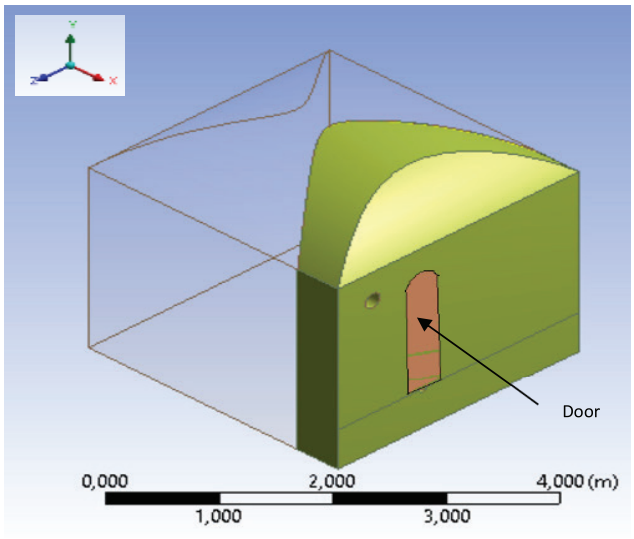

Figure 7. Shelter with a closed door.

feeds the extractor operation. In this case, the effects of two air velocity values at the extractor level are studied (V_1 = 1 *m/s*, V_2 = 0.5 *m/s*).

Habitually, in this rural area, firewood embers are used for night heating. There are other modern devices for solar energy storage. The recommended modes encompass hydrogen [27] and compressed air systems [28], which convert stored fluids into electricity. But, they are still costly for small-size power.

RESULTS AND DISCUSSION

The mathematical model is validated, and three shelter cases are analyzed: the base case, the case with a closed door, and the case with a PVT solar collector. The effects on indoor air temperature and velocity inside the shelter are investigated.

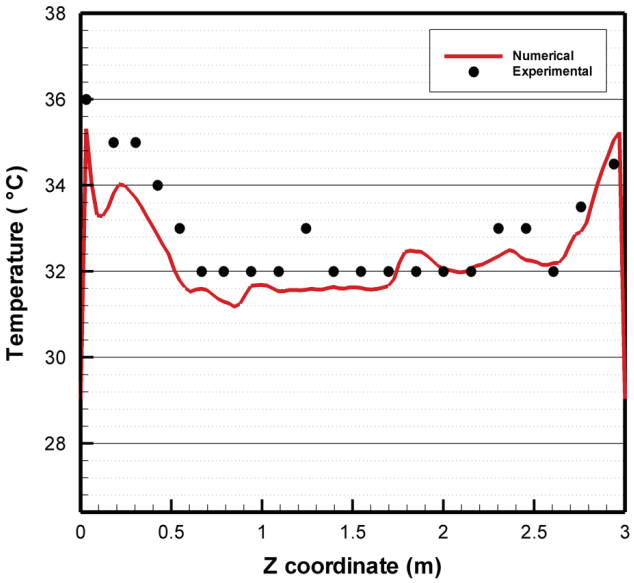

Figure 9. Numerical and experimental temperatures at shelter median line.

Model Validation

On August 9th, 2022, the temperature on the shelter median line was collected and used as a validation reference. Figure 9 shows the numerical results compared to the experimental data. Generally, a good agreement is observed where the maximal value of the relative error is less than 4.6%.

Shelter Base Case

In this case, the shelter is simulated in its original state without any alterations. The lowest ambient temperature in 2022 is 3.5°C for all cases, as determined by the Meteonorm code, and is recorded on January 12th, 2022. The analysis focuses on investigating the thermal and dynamic fields.

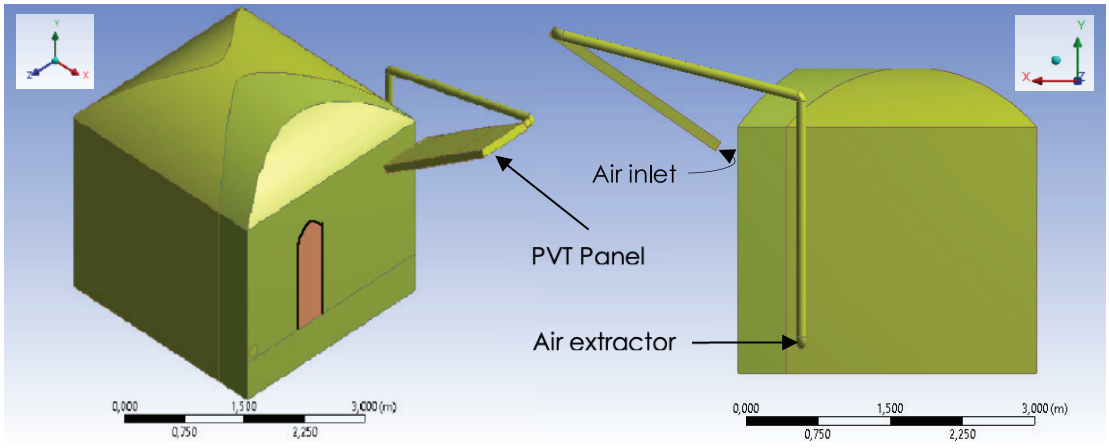

Figure 8. Shelter with PVT collector.

Thermal field

Figures 10 and 11 show the shelter air temperature contours in transversal planes at (Z = 0.4; 1.7; 2.85 m) and longitudinal planes at (X = -0.5; -2.2 m), respectively.

A drop in temperature is observed at the shelter entrance due to the absence of a door, allowing cold air to enter the shelter. Figure 12 shows the temperature variation along the shelter's central axis at a height of 0.6 m in the longitudinal direction (Z). The figure illustrates that the temperature along this line does not rise above 10°C. This temperature level indicates an uncomfortable thermal condition inside the shelter. For increasing the temperature at the entrance, a new shelter design incorporating a separating door is necessary to reduce the influence of ambient cold air.

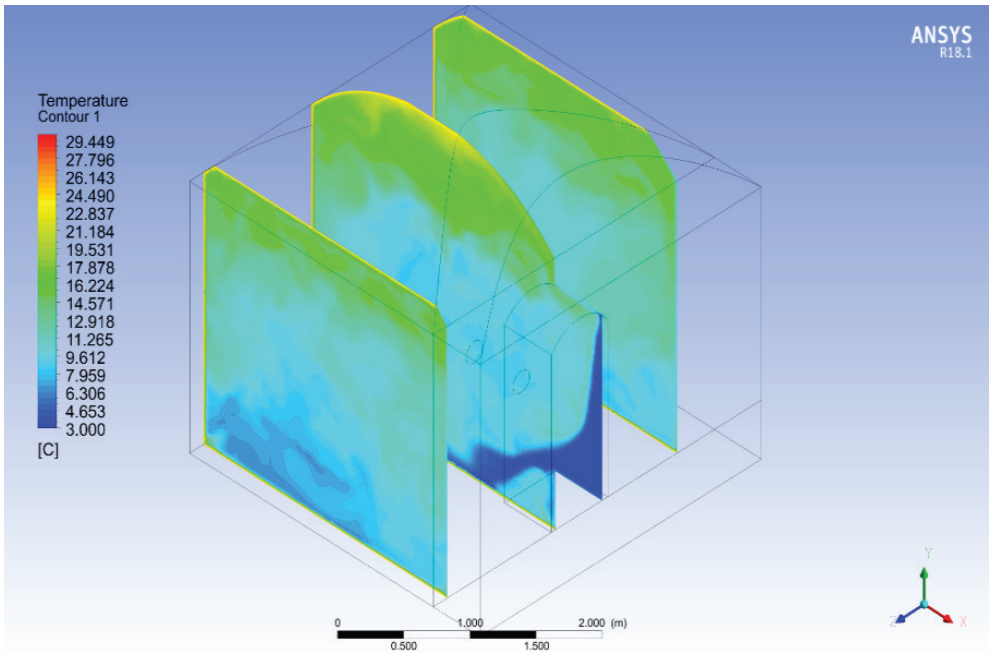

Figure 10. Temperature contours in transversal planes.

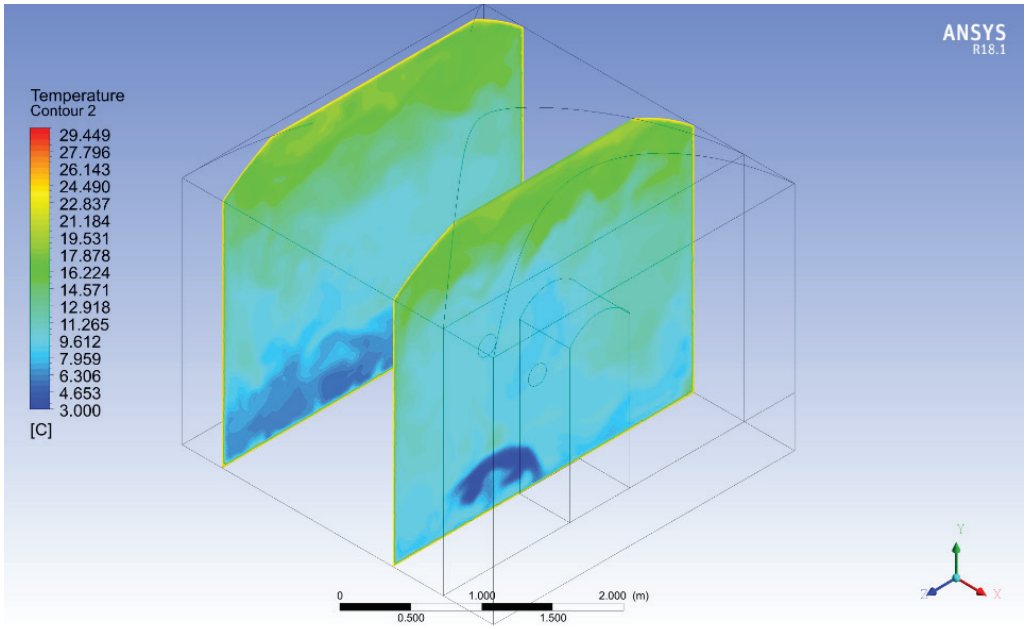

Figure 11. Temperature contours in longitudinal planes.

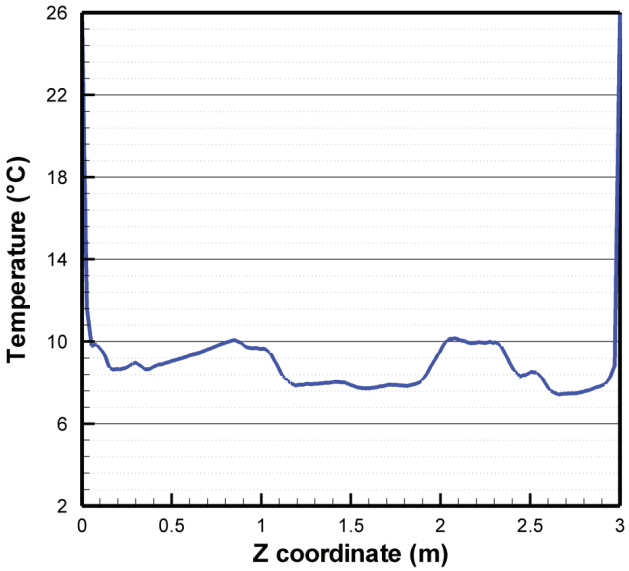

Figure 12. Shelter temperature on median line.

Dynamic field

Concerning the velocity field, Figure 13 presents the air velocity contours in the transversal planes at $Z = 0.4; 1.7; 2.85$ *m*. In general, the air velocity is too low, with a slight increase near the door due to the infiltration of ambient cold air, leading to a limited achievement of thermal comfort.

Shelter with Closed Door

In this case, a wooden door is installed to seal the shelter, featuring a small hole underneath to minimize infiltrating the cold air while maintaining shelter ventilation. The air temperature and velocity fields are investigated as follows:

Thermal field

Figures 14 and 15 show the shelter air temperature contours in the same planes presented in the previous case. They illustrate a relative enhancement in thermal comfort in terms of temperature levels and distribution, along with a notable increase in indoor temperature compared to ambient air. In Figure 16, the temperature exceeds 21°C along the same central line mentioned previously, representing a temperature difference of 11°C between the two cases. The difference between indoor and ambient temperatures amounts to 18°C, a substantial achievement in thermal comfort, achievable through a simple modification to the shelter. However, further thermal enhancements can be achieved by harnessing solar energy, a free and environmentally friendly source. This modification will be explored in the subsequent case.

Dynamic field

Figure 17 shows air velocity contours in the same planes as the previous case. A low air velocity reigns on most of the shelter area, contributing to additional thermal comfort.

Shelter with a PVT collector

Passive heating using solar systems is low-cost and environmentally friendly and can meet a large portion of the building heating demand. This technique is added to the previous case modification; it consists of introducing a PVT solar collector. The aeration hole is relocated to a

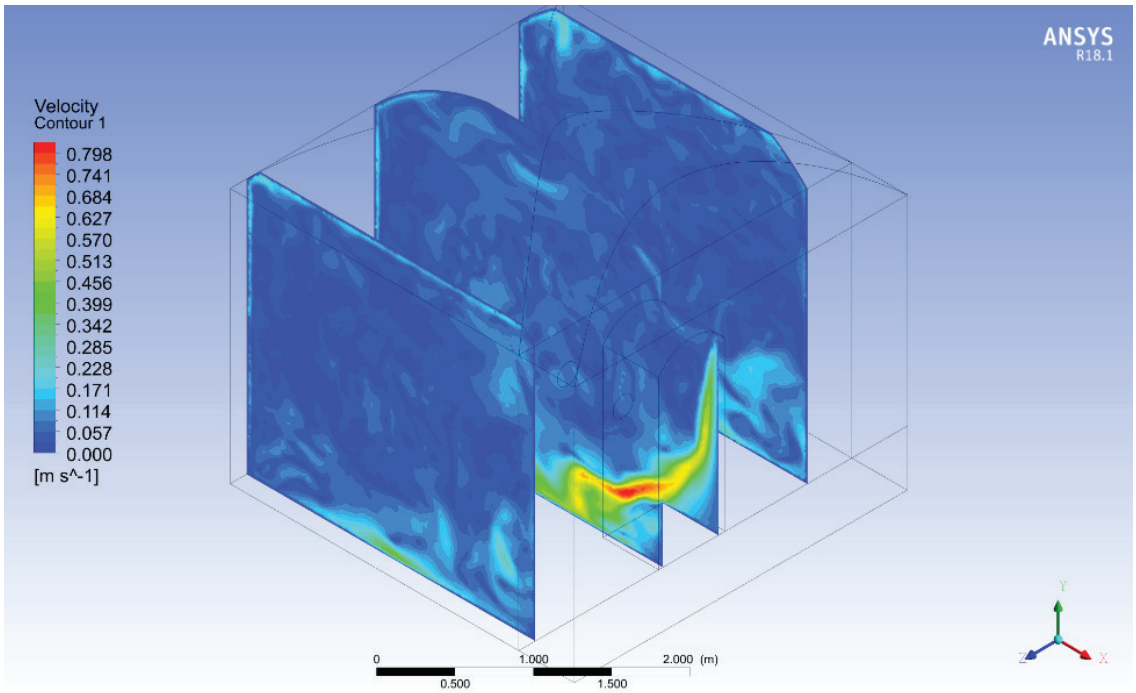

Figure 13. Air velocity contours in transversal planes.

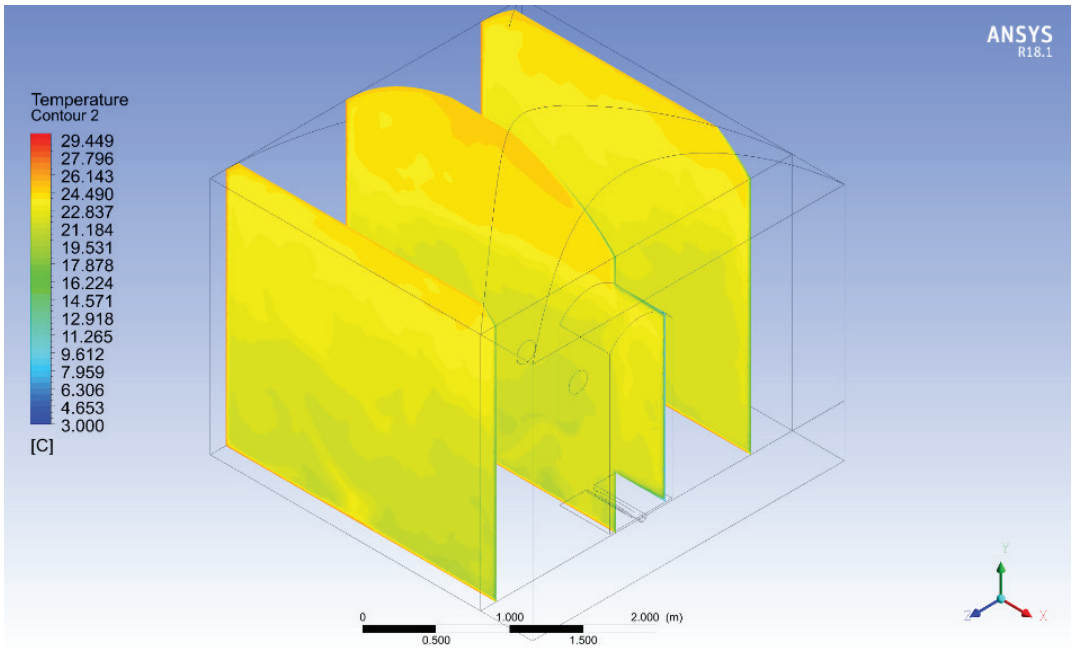

Figure 14. Temperature contours in transversal planes.

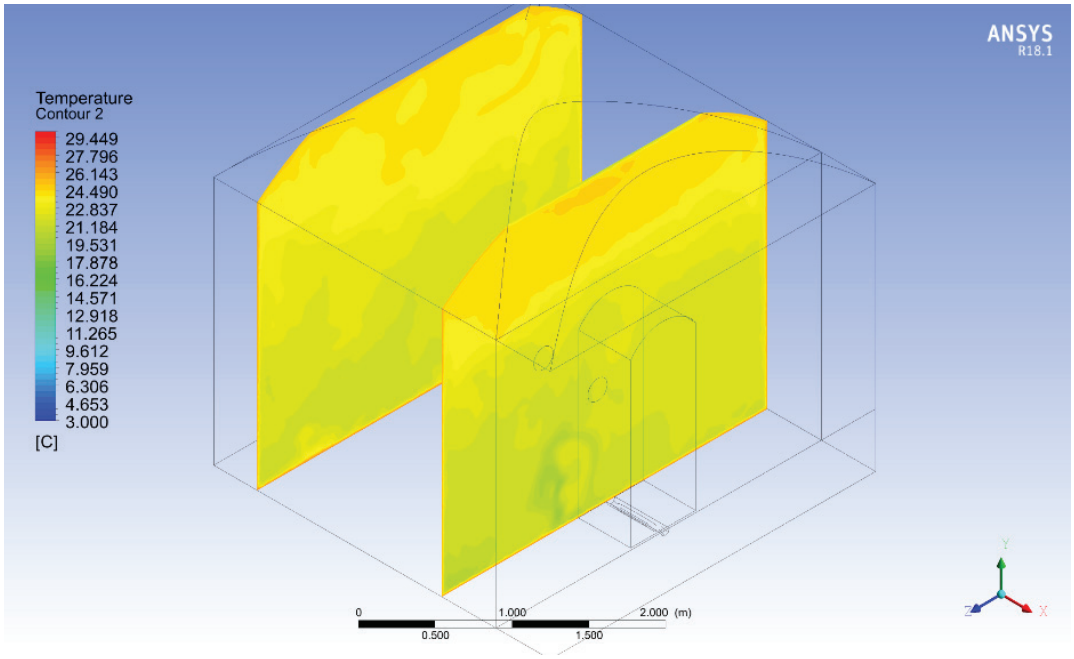

Figure 15. Temperature contours in longitudinal planes.

lower position to evacuate cold air. This case is investigated in two variants according to the air velocity applied at the extractor level ($V_1 = 1$ *m/s* and $V_2 = 0.5$ *m/s*).

First variant ($V_1 = 1$ *m/s*)

a) Thermal field: Figures 18 and 19 show the shelter air temperature contours in the same planes presented in the previous case. In Figure 20, the curve indicates an increase in indoor temperature, exceeding 23°C, marking a rise of approximately two degrees compared to the previous case.

b) Dynamic field: Figure 21 presents the air velocity contours in the same transversal planes as the previous case. Most of the sheltered area experiences no air velocity except near the air inlet and outlet. This aeration contributes to achieving good thermal comfort.

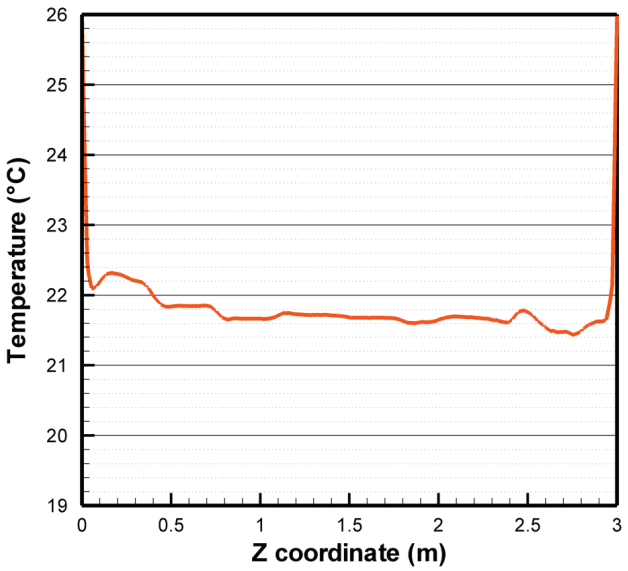

Figure 16. Shelter temperature on median line.

Second variant (V_2 = 0.5 *m/s*)

a) Thermal field: In this variant, the air inlet velocity is halved compared to the previous variant. Figures 22 and 23 present the shelter air temperature contours in the same transversal and longitudinal planes chosen in the precedent cases. The results indicate a high increase in room temperature compared to the precdent variant. Additionally, Figure 24 suggests that the temperature generally rises by approximately 1°C along the median line of the shelter.

b) Dynamic field. Figure 25 illustrates the air velocity contours in the same transversal planes as the previous variant. The air velocity records an additional increase over most shelter space compared to the previous variant. Consequently, this variant can potentially achieve more thermal comfort.

Comparison Between the Different Cases

The thermal fields of the different cases are compared, including the base case (case 1), the shelter with a closed door (case 2), and the shelter with a PVT collector (case 3). Figure 26 summarizes the median line temperature of the shelter at a height of 0.6 m along the Z axis. It reveals a temperature difference of approximately 15°C between the first and last variants of the third case. This suggests that simple modifications made to the original shelter can effectively use a PVT solar collector for heating in a cold desert climate.

Economic Approach

During the cold period in Algeria, the heat pump is the most used device to heat off-grid buildings. The minimal calorific power to heat a standard room is 12,000 BTU (3.5 kW) [29]. Generally, the heat pump COP relies on between 2.5 and 7 [30]. By applying a low COP (2.5), the electric power of the heat pump compressor is 1.4 kW, neglecting their fan consumption. Also, to achieve good heat pump performance needs installing the evaporator in an underground location which requires additional space and construction [31]. However, the heating of this shelter by a PVT collector requires only an air extractor with an electric power extending from 0.375 to 0.405 kW [29]. Therefore,

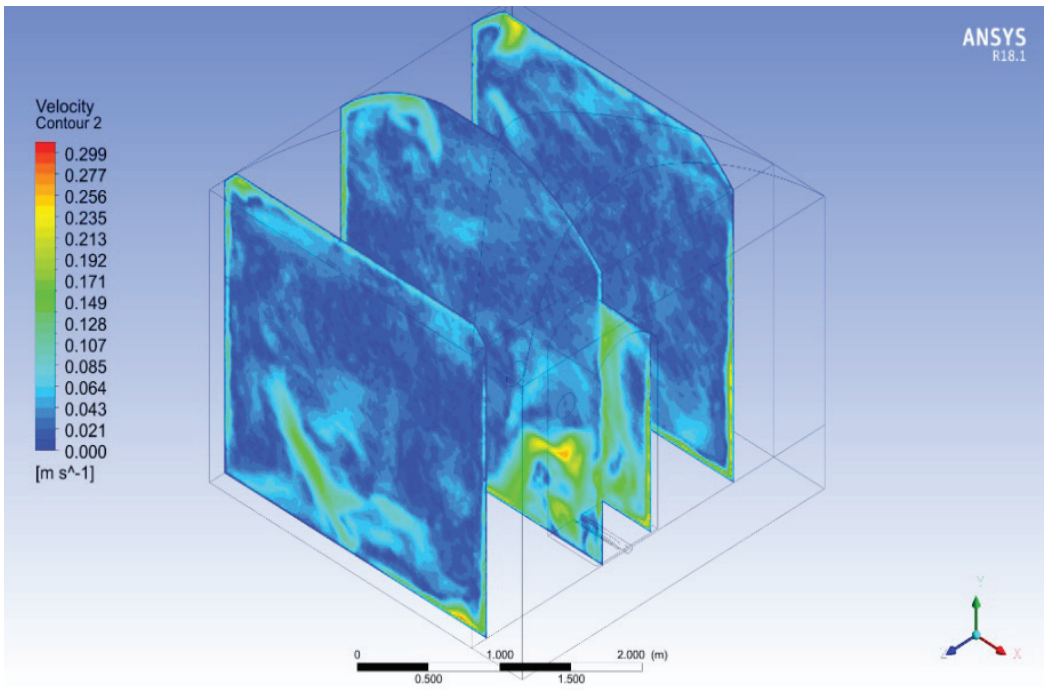

Figure 17. Air velocity contours in transversal planes.

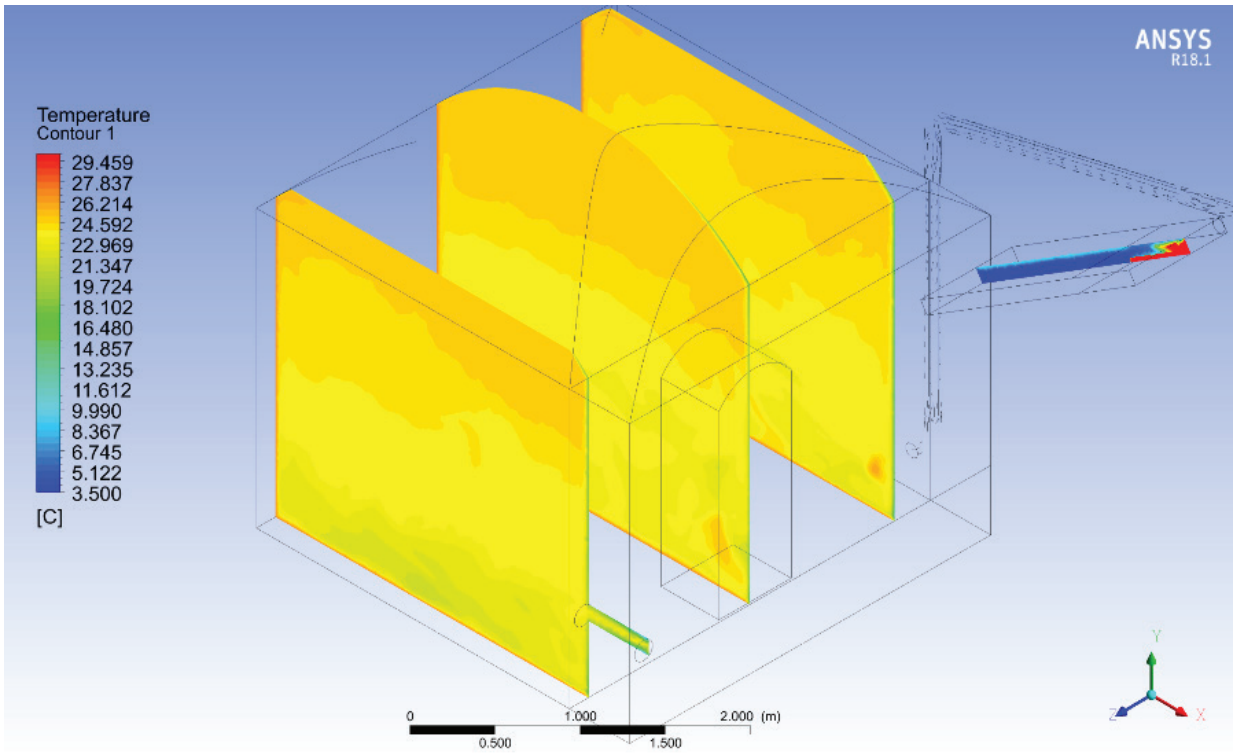

Figure 18. Temperature contours in transversal planes.

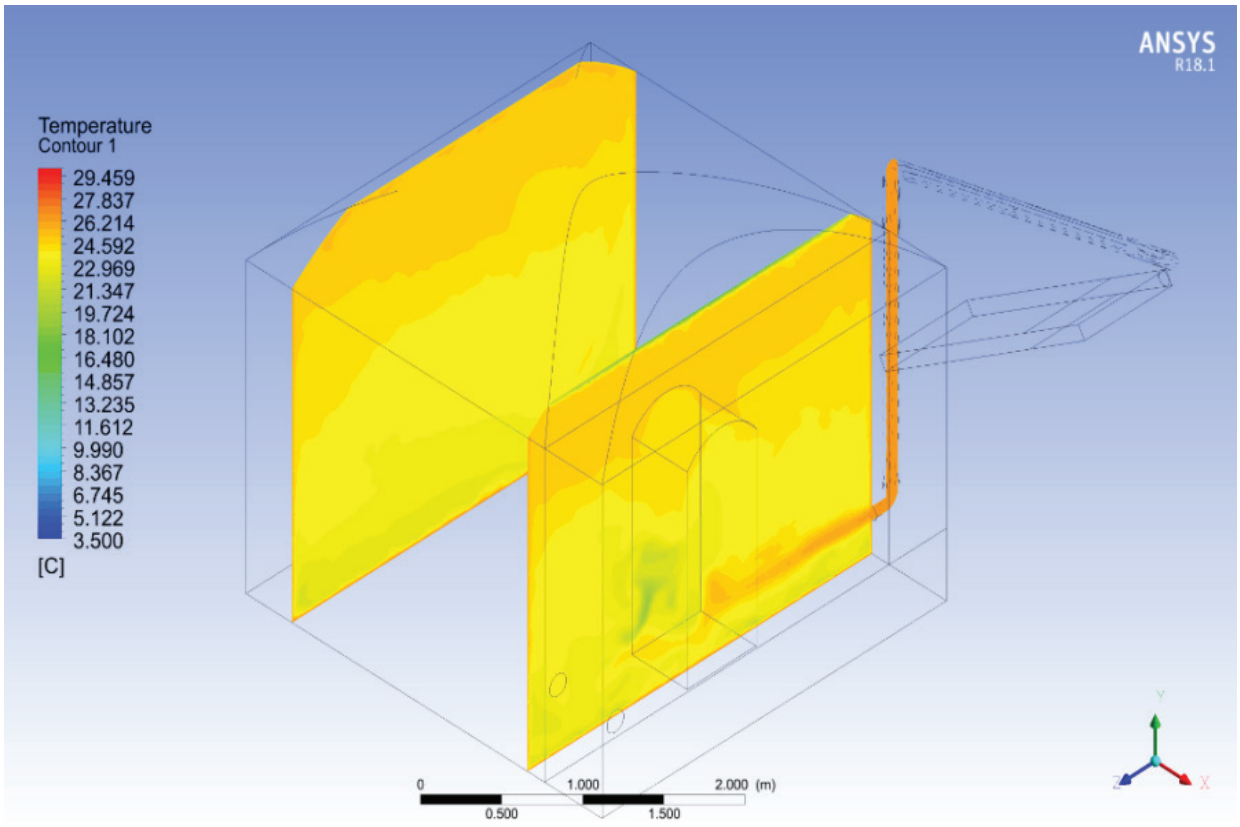

Figure 19. Temperature contours in longitudinal planes.

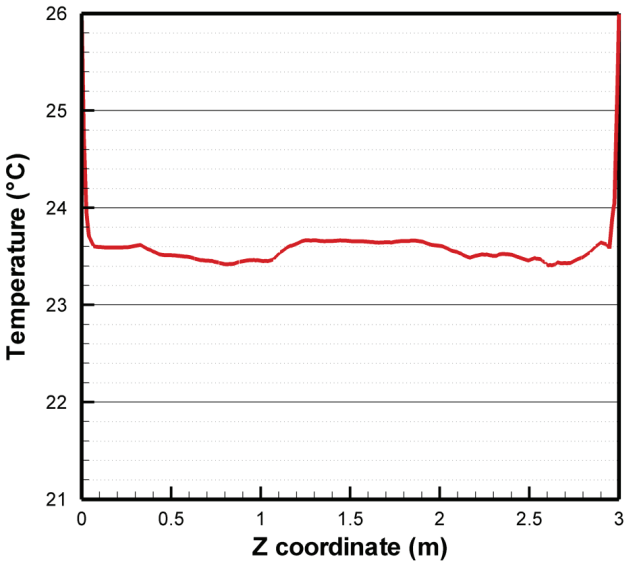

Figure 20. Shelter temperature on median line.

at least the PVT system cost presents only 30% of the compared heat pump system. The PV peak power model [27] shows that the heat pump requires a PV panel evaluated at 1500 W, while the PVT collector needs only a PV panel of 300 W.

The initial cost evaluation is based on the prospection of the local market and the use of the currency exchange of Dinar Algerian (DZD) to Euro (1 Euro=150 DZD). The price of a 12,000 BTU heat pump is 470 Euros, and its operation needs a PV panel of 1350 Euros.

Concerning the PVT system, a cost assessment based on the metallic support, Zinc pipes, air extractor, wooden air canal, PV panel and command system is performed where the initial global cost reaches about 360 Euros. So, the gap between the two investments is 1460 euro. It is noted that the maintenance cost of the heat pump is higher than the PVT system, which will further increase the gap. All these reasons make the discovered façade shelter-PVT system more advantageous than the heat pump for heating purposes.

Including the different palm kinds, the harvesting palm period extends for three months. The transportation between the farm and the city is evaluated to show the exploitation profit of this discovered façade shelter. Two methods can be used for the daily transport of two workers along the 20 km separating the farm and the city:

- The farm owner can buy a lightweight car for 10000 euros. The annual car fuel consumption and maintenance reaches 2400 euros,
- The farm owner rents a taxi car with 2100 euros for the year harvesting period.

The use of the discovered façade shelter needs only the transportation rent of the workers for twelve times during the year harvesting period with 280 euros. According to the study of M. Lacheheb and Sirag [32], generally, in Algeria, the inflation rate depends on the oil exportation price. However, local products and services like fuels and transportation have a slight annual price increase of about 3%.

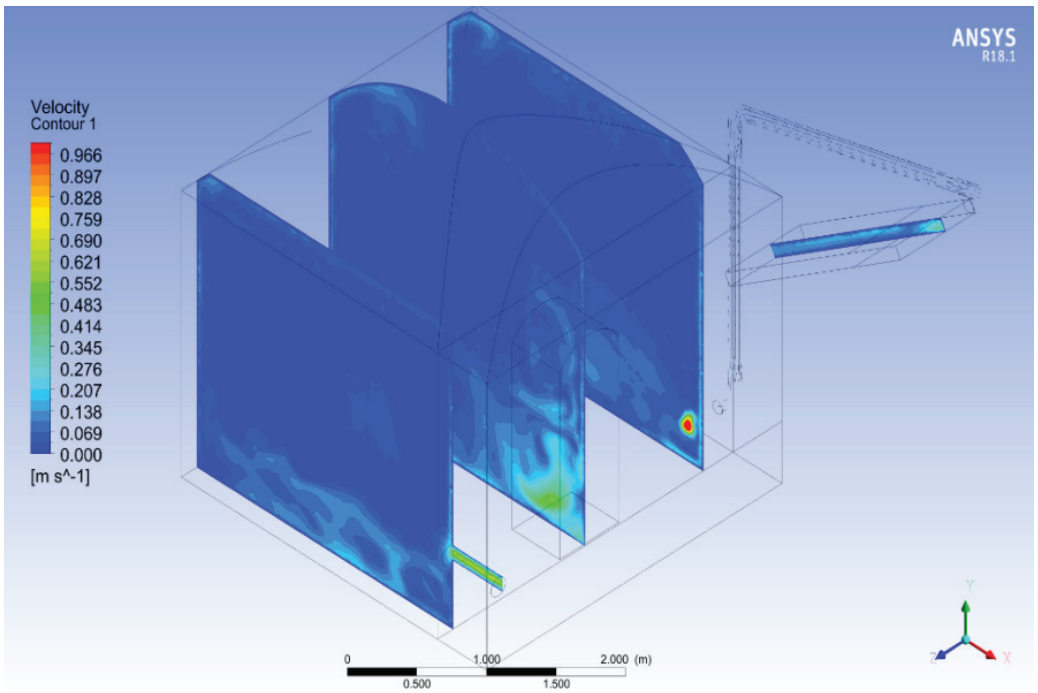

Figure 21. Air velocity contours in transversal planes.

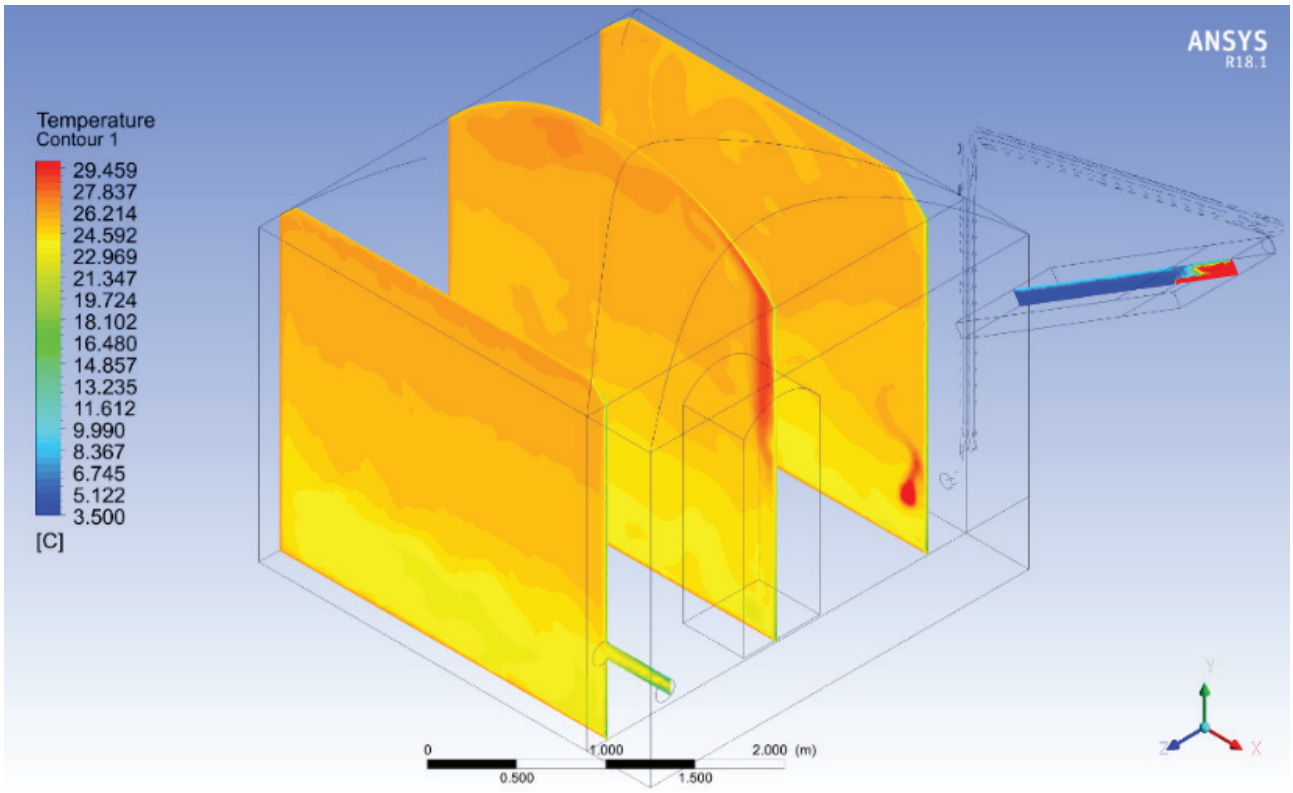

Figure 22. Temperature contours in transversal planes.

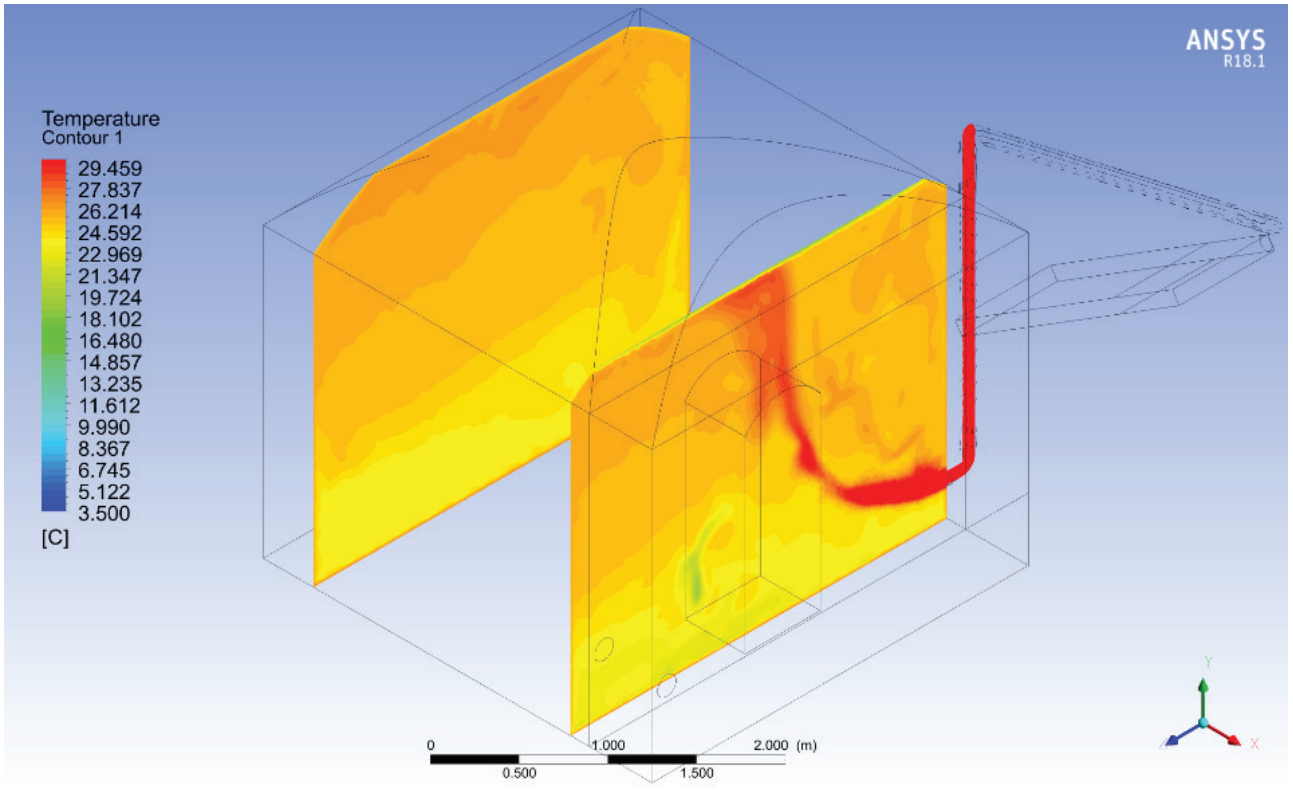

Figure 23. Temperature contours in longitudinal planes.

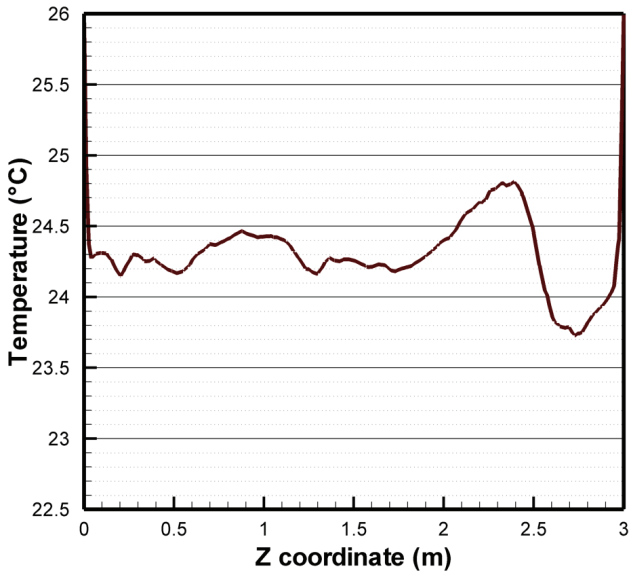

Figure 24. Shelter temperature on the median line.

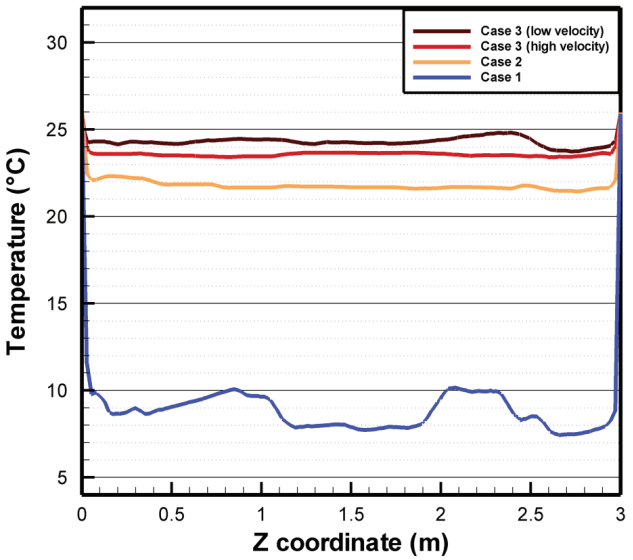

Figure 26. Temperature on median line for all cases.

After ten years, this transportation rent reaches about 10% and 15% compared to the first and second variants (Fig. 27). Also, this agricultural zone contains 22 shelters that can be exploited. So, the discovered façade shelter-PVT system presents a significant benefit compared to the second and first variants; it reaches 10000 and 30000 euros, respectively. These money amounts can be oriented to other investments for developing palm tree agriculture.

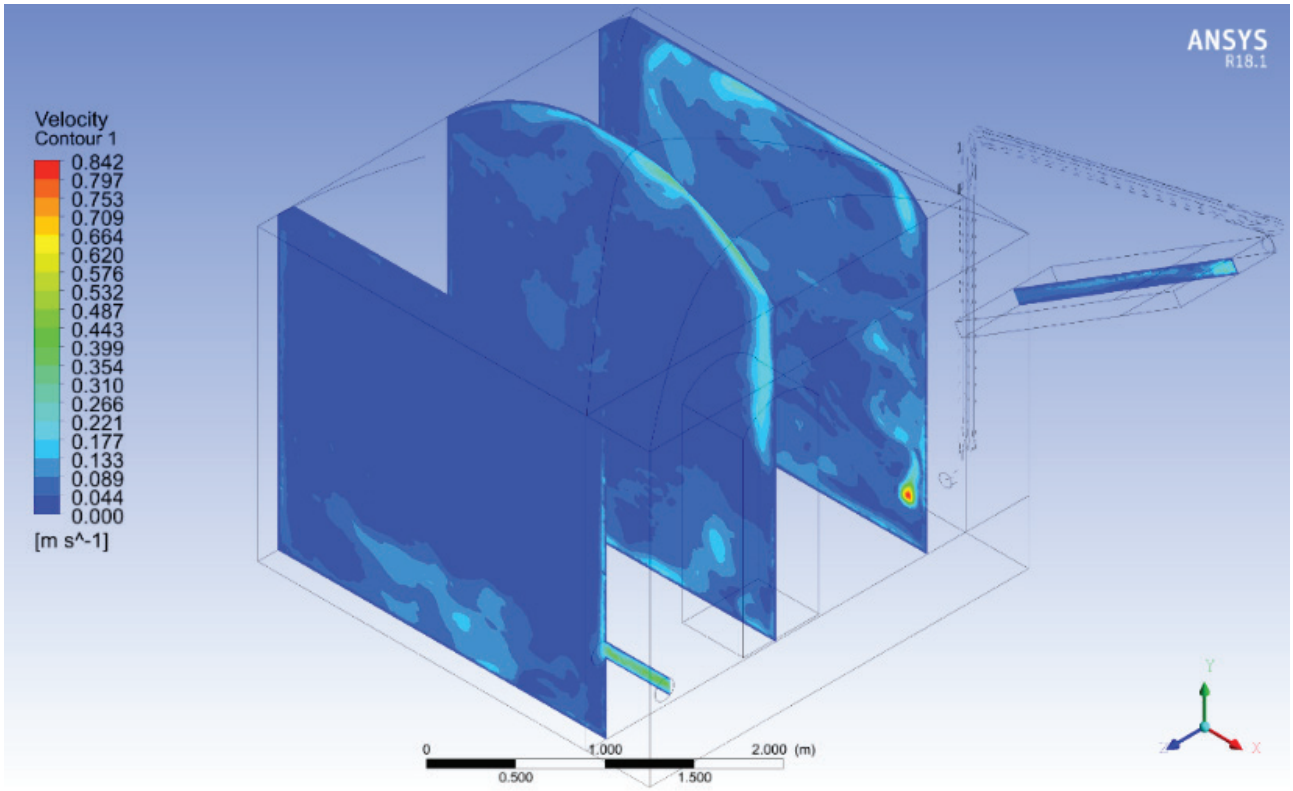

Figure 25. Air velocity contours in transversal planes.

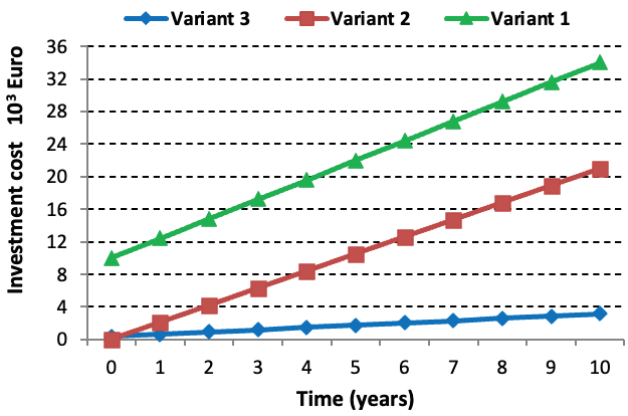

Figure 27. Comparison between the three variants.

CONCLUSION

The thermal behavior for heating a revealed façade shelter in a desert climate is examined by conducting a three-dimensional airflow simulation using ANSYS code. The main paper conclusions are assigned in the following items:

- The base case shelter temperature is improved by adding a wooden door at the shelter entrance; where the indoor temperature reaches about 18°C with an ambient temperature of 3.5°C.
- By adding a PVT collector and an air extractor, the indoor temperature reaches 24°C, and a high temperature is achieved for a low inlet air velocity at the air extractor level. This parameter level presents good thermal comfort for shelter occupants.
- The initial investment cost gap between a heat pump and the proposed system is 1460 euros, and the high heat pump maintenance can provide a supplementary gap increase. In addition, the long-term investment cost shows that the discovered façade shelter operation can provide 30000 euros as profit compared to the first variant of the workers' transportation method.

Despite the significant advantages of the discovered façade shelter, its exploitation stays relatively limited due to the lack of hills in certain southern Algerian cultural areas.

AUTHORSHIP CONTRIBUTIONS

Authors equally contributed to this work.

DATA AVAILABILITY STATEMENT

The authors confirm that the data that supports the findings of this study are available within the article. Raw data that support the finding of this study are available from the corresponding author, upon reasonable request.

CONFLICT OF INTEREST

The authors declared no potential conflicts of interest with respect to the research, authorship, and/or publication of this article.

ETHICS

There are no ethical issues with the publication of this manuscript.

REFERENCES

[1] Chan H, Riffat SB, Zhu J. Review of passive solar heating and cooling technologies. Renew Sustain Energy Rev 2010;14:781–789. [CrossRef]

[2] Elghamry R, Hassan H. Experimental investigation of building heating and ventilation by using Trombe wall coupled with renewable energy system under semi-arid climate conditions. Sol Energy 2020;201:63–74. [CrossRef]

[3] Dong J, Chen Z, Zhang L, Cheng Y, Sun S, Jie J. Experimental investigation on the heating performance of a novel designed Trombe wall. Energy 2019;168:728–736. [CrossRef]

[4] Buker MS, Riffat SB. Building integrated solar thermal collectors – A review. Renew Sustain Energy Rev 2015;51:327–346. [CrossRef]

[5] Agathokleous R, Barone G, Buonomano A, Palombo A. Building façade integrated solar thermal collectors for air heating: experimentation, modelling and applications. Appl Energy 2019;239:658–679. [CrossRef]

[6] Buonomano A, Forzano C, Kalogirou SA, Palombo A. Building-façade integrated solar thermal collectors: energy-economic performance and indoor comfort simulation model of a water-based prototype for heating, cooling, and DHW production. Renew Energy 2018;137:20–36. [CrossRef]

[7] Li Q, Zheng C, Shirazi A, Taylor RA. Design and analysis of a medium-temperature, concentrated solar thermal collector for air-conditioning applications. Appl Energy 2017;190:1159–1173. [CrossRef]

[8] Miao R, Hu X, Yu Y, Zhang Y, Wood M, Olson G. Experimental study of a newly developed dual-purpose solar thermal collector for heat and cold collection. Energy Build 2021;252:111370. [CrossRef]

[9] Maurer C, Baumann T, Hermann M, Lauro PD, Pavan S, Michel L, et al. Heating and cooling in high-rise buildings using facade-integrated transparent solar thermal collector systems. J Build Perform Simul 2013;6:449–457. [CrossRef]

[10] Monghasemi N, Vadiee A. A review of solar chimney integrated systems for space heating and cooling application. Renew Sustain Energy Rev 2017;81:2714–2730. [CrossRef]

[11] Haghighi AP, Maerefat M. Solar ventilation and heating of buildings in sunny winter days using solar chimney. Sustain Cities Soc 2014;10:72–79. [CrossRef]

[12] Hong S, Maerefat M. Annual energy performance simulation of solar chimney in a cold winter and hot summer climate. Build Simul 2019;12:847–856. [CrossRef]

[13] Li Y, Liu S. Numerical study on thermal behaviors of a solar chimney incorporated with PCM. Energy Build 2014;80:406–414. [CrossRef]
[14] Mohammed FZ, Hussein AM, Danook SH, Barhm M. Characterization of a flat plate solar water heating system using different nano-fluids. AIP Conf Proc 2023;2901:100018. [CrossRef]
[15] Qader FF, Mohammed FZ, Barhm M. Thermodynamic analysis and optimization of flat plate solar collector using TiO2/Water nanofluid. J Harbin Inst Technol New Ser 2023:2023050.
[16] Qader FF, Mohamad B, Hussein AM, Danook SH. Numerical study of heat transfer in circular pipe filled with porous medium. Pollack Period 2023;19:137–142. [CrossRef]
[17] Simplemaps. Algeria Cities Database. Available at: https://simplemaps.com/data/dz-cities. Accessed Jul 22, 2021.
[18] World Meteorological Organization. World Weather Information Service. Available at: http://worldweather.wmo.int/en/city.html?cityId=1436. Accessed Jul 22, 2021.
[19] Weather Spark. Climate and Average Weather Year Round in Ouargla Algeria. Available at: https://weatherspark.com/y/51500/Average-Weather. Accessed Jul 24, 2021.
[20] Giorgini GD. The validity of the Boussinesq approximation for liquids and gases. Int J Heat Mass Transf 1975;19:545–551. [CrossRef]
[21] Messaoudi MT, Dokkar B, Khenfer N, Benzid MC. 3D investigation of semi-underground room comfort in a desert climate. J Therm Eng 2021;7:1577–1590. [CrossRef]
[22] Cherrad I, Dokkar B, Khenfer N, Benoumhani S, Benzid MC. Cooling improvement of an agricultural greenhouse using geothermal energy in a desert climate. Int J Energy Environ Eng 2021;14:211–228. [CrossRef]
[23] Belatrache D, Bentouba S, Bourouis M. Numerical analysis of earth air heat exchangers at operating conditions in arid climates. Int J Hydrogen Energy 2017;42:8898–8904. [CrossRef]
[24] Derbal HB, Kanoun O. Investigation of the ground thermal potential in Tunisia focused towards heating and cooling applications. Appl Therm Eng 2010;30:1091–1100. [CrossRef]
[25] Alloui I, Ben Moussa H, Vasseur P. Soret and thermosolutal effects on natural convection in a shallow cavity filled with a binary mixture. Int J Fluid Flow 2010;31:191–200. [CrossRef]
[26] Khenfer N, Dokkar B, Messaoudi MT. Overall efficiency improvement of photovoltaic thermal air collector: numerical and experimental investigation in the desert climate of Ouargla region. Int J Energy Environ Eng 2020;11:497–516. [CrossRef]
[27] Dokkar B, Negrou B, Settou N, Imine O, Chennouf N, Benmhidi A. Optimization of PEM fuel cells for PV-hydrogen power system. Energy Procedia 2013;36:798–807. [CrossRef]
[28] [Messaoudi Y, Cherrad N, Dokkar B, Halimi S, Boudjelab F, Saidani Y, Senouci F, Belloufi A, Aliouat K, Mezoudj M. Power control of PV and grid-assisted CAES system integrated into SONATRAC HLP GSP1 ELR1 pumping station with thermal. Energy Convers Manag 2023;294:117563. [CrossRef]
[29] Messaoudi MT, Dokkar B, Khenfer N, Benzid MC. Multi-criteria optimization of a geothermal system used for indoor refreshment during summer in a hot region. Int J Environ Sci Technol 2023;20:9571–9586. [CrossRef]
[30] Pospísil J, Spilacek M, Kudela L. Potential of predictive control for improvement of seasonal coefficient of performance of air source heat pump in Central European climate zone. Energy 2018;154:415–423. [CrossRef]
[31] Kumar B. Fossil energy reduction for heating and cooling of buildings using shallow geothermal integrated energy systems – a comprehensive review. J Therm Eng 2023;9:1386–1417. [CrossRef]
[32] Lacheheb M, Sirag A. Oil price and inflation in Algeria: A nonlinear ARDL approach. Q Rev Econ Finance 2019;73:217–222. [CrossRef]
[33] Saifi N, Settou N, Dokkar A. Modeling and parametric studies for thermal performance of an earth to air heat exchanger in South East Algeria. 6th Int Renewable Energy Congress IREC2015, 24-26 March 2015, Sousse, Tunisia. pp. 1–6. [CrossRef]
[34] Ozel M. Determination of optimum insulation thickness based on cooling transmission load for building walls in a hot climate. Energy Convers Manag 2013;66:106–114. [CrossRef]
[35] Ozel M, Ozel C. Comparison of thermal performance of different wall structures. HEFAT2012 9th International Conference on Heat Transfer, Fluid Mechanics and Thermodynamics, 16-18 July 2012, Malta. pp. 674–679.

APPENDIX

The boundary conditions temperature:

$$T(z,t) = T_{mean} + A\cos\left[\omega(t - t_0) - \frac{z}{d}\right]\exp\left(-\frac{z}{d}\right) \quad (1)$$

Where:

- T_{mean}: The mean annual soil temperature.
- A: The amplitude from the soil surface temperature.
- $\omega=2\pi/P$, where P is the period of the sinusoid.
- t: The time coordinate. (t = 0 from 1 January at 0 s).
- t_0: The phase constant (time of maximal soil surface temperature).
- Z: The depths coordinate.
- $d = (2\alpha/\omega)^{0.5}$, where α is soil thermal diffusivity:

$$\alpha=\lambda_{soil}/(\rho_{soil}.C_{p\,soil}) \quad (2)$$

The underground temperature model is validated against the experimental data measured in Ouargla City by Saifi et al. [33].

Concerning the façade's external surface temperature, it is determined using the following relation [34]:

$$T_e = T_0 + \frac{\alpha.I_T}{h_0} - \frac{\varepsilon\Delta R}{h_0} \quad (3)$$

With:

- T_e: External surface temperature.
- T_0: Ambient temperature.
- $\frac{\alpha}{h_0}$: Absorption capacity rate of outer surface $0.026 \le \frac{\alpha}{h_0} \le 0.052$ [35].
- h_0: A correction factor (4°C for horizontal and 0°C for vertical surfaces).
- I_T: Total solar radiation.

The construction material of the shelter is the cohesive soil of the hill. The air and the soil thermo-physical properties are shown in suppl. Table 1.

Supplementary Table 1. Thermo-physical properties of the air and the soil

Material	Density (kg/m³)	Thermal capacity (J/kgK)	Thermal conductivity (W/mK)
Air	1.1774	1005.7	0.02624
Cohesive soil [22]	2050	1840	0.52